LAMINAR NATURAL CONVECTION IN HORIZONTAL ANNULAR SEGMENTS

M.A. Hassab, S.M. ElSherbiny and Kh.Y. Zakaria
Mechanical Engineering Department, Faculty of Engineering,
Alexandria University, Alexandria, Egypt

ABSTRACT

A numerical solution of the mass, momentum and energy equations was given for the laminar natural convection in horizontal annular segments. The differential equations were transformed to finite difference equations using a central differencing scheme except for the convection term where a power-law scheme was used as described in the SIMPLE method. An irregular grid of 50x40 (r x θ) was used. The effect of variable properties was investigated and the Boussinesq assumption resulted in a reduction in the estimated Nusselt numbers. Isotherms and stream lines were given to explain the effect of rotation on flow regimes. A minimum value of Nu was observed at different values of the angle of rotation as the radii ratio was changed. The effects of radii ratio, Rayleigh and Prandtl numbers on the average Nusselt number were given in correlations for different values of the angle of rotation.

Keywords: Heat transfer natural convection, Convection in annular segments.

1. INTRODUCTION

Natural convection in horizontal annuli has been the subject of interest for the past 25 years and many experimental, analytical and numerical papers have appeared in the literature. The importance of the problem came from its appearance in many important applications such as insulation of underground pipe-in-pipe systems, electronic cooling, aircraft cabin insulation, solar collectors design, nuclear reactors design, etc. Under certain circumstances, the convection needs to be suppressed or minimized in the annulus and thus may become one of the important considerations in the design process.

Comprehensive and excellent reviews of the investigations up to 1976 have been given by Kuehn and Goldstein [1]. In recent years, studies have been made concerning high Rayleigh number range [2], concentric and eccentric horizontal cylindrical annuli with and without rotation [3-6], effect of variable properties [7-8], mixed boundary conditions [9], other physical effects [10-14], three-dimensionality [15-17], density inversion [18] and transient responses [19-20].

Farouk and Güceri [2] presented numerical solutions for Ra_l ranging from 10^6 to 10^7 with a K-ϵ turbulence model and a radii ratio of 2.6. They also accounted for the buoyancy effects on the turbulence structure. The results for both the laminar and turbulent cases are in good agreement with experimental data. Cho et al [5] used a bi-polar coordinates system to investigate the local and overall heat transfer between concentric and eccentric horizontal cylinders for a range of Rayleigh number less than 5.0×10^4 based on the difference of radii. They found that the case of very small eccentricity ($\leq$ 0.01) gives an overall thermal behavior similar to that of the exactly concentric cylinders.

Prusa and Yao [6] used a radial transformation to map the eccentric outer boundary into a concentric circle. They found that eccentricity influences the flow in two ways. First, by decreasing the distance between the two cylinders over part of their surfaces, it increases the local heat transfer due to conduction.

Second, the eccentricity influences the convective mode of heat transfer. Results show that moderate positive values of eccentricity, enhance convective heat transfer.

Mahony et al [7], and Hessami et al [8] investigated the effect of variable properties on natural convection in horizontal annulus, they found that the Boussinesq approximation is valid for a temperature difference ratio $\xi = (T_h-T_c)/T_c < 0.1$ but can be used for a ratio up to 0.2 with reasonable accuracy. They also found that the Boussinesq approximation does overestimate the tangential velocity and the temperature gradient near the hot inner cylinder .

Kumar [9] presented the numerical results for the case of constant heat flux at the inner cylinder and isothermal condition at the outer cylinder. A lower effective sink temperature is obtained when it is compared to isothermal heating, thus a higher heat transfer rate is expected.

Hessami et al [14] studied experimentally and theoretically the effect of changing the fluid properties within the annulus on natural convection mode. They used air, glycerin and mercury, and showed that glycerin is more sensitive to the constant properties assumption, while air had not been significantly affected by this assumption. This is due to the large radii ratio they used ($\gamma=d_o/d_i=11.0$). Finally, the experimental data have been correlated with some other data from the literature for smaller values of γ, and it has been shown that the heat transfer from the inner cylinder should be almost the same as that in an infinite medium when $\gamma \geq 10$.

Rao et al [15] investigated numerically and experimentally the flow in horizontal concentric annuli with emphasis on the various flow patterns, with two-and three-dimensional calculations over a range of Rayleigh number and radii ratio. The transition to the multicellular flow pattern which has been observed by Powe et al [16] is confirmed, and an oscillating flow is generated at the upper part of the annulus as Rayleigh number increases.

Clearly, most of the investigations considered so far are for the plain annuli. A few investigations are on annuli with radial spacers [21] or with various transverse fins [22] or annulus with azimuthal baffles [23]. Kwon et al [21] studied, both theoretically and experimentally, convection in an annulus with three equally spaced axial spacers. A spacer made of material with low thermal conductivity reduces heat transfer by as much as 20%, while the one with high conductivity suppresses the natural convection heat transfer between the cylinders. Good agreement with experimental data for temperature distribution and local heat transfer coefficient was obtained. The studies by Kwon and Kuehn [22] are for horizontal cylinders in the infinite medium with conducting plate fins and transverse circular fins. The study of Yang and others [23] was on natural convection suppression in horizontal annuli by azimuthal baffles. They used a general orthogonal coordinates system and a basic control volume approach. Aiming to study the possible suppression of convection by azimuthal baffles, they placed the baffles at top, central, and bottom regions of the annular gap. The study covered a wide range of Rayleigh number (1.2×10^2 - 10^6) and radii ratio (1.4-4). The gap fluid was air and variable fluid properties were observed. The most efficient way of reducing heat transfer is the case where the baffle prevents direct flow into the inner and outer cylinders. An increase of heat transfer occurs when the baffles are at the position where the crescent-shaped streamlines are stretched . Only a small reduction in heat transfer is obtained when the baffle is placed in the stagnant region of the annulus.

From this review we can conclude that no previous work was found for the problem of natural convection in a cylindrical annular segment and only a little work was done in similar problems. So, our basic aim here is to solve this problem to get the complete image about the heat transfer characteristics of this problem.

2. THEORETICAL ANALYSIS

In the present study we will investigate the effect of the following parameters on the heat transfer behavior of laminar free convection inside the horizontal annular segment shown in Figure (1).

i- The gap Rayleigh number Ra_{d_i}, in the range from 10^3 to 10^6.

ii- The gap radii ratio, $\gamma = d_o/d_i$ in the range from 2.0 up to 6.0.

iii- The angle of rotation ω from a vertical plane, which was varied from vertical position ($\omega=0^o$) to horizontal position ($\omega=90^o$).

iv- The sector angle, ζ which was changed from 90^o to 300^o.

v- Prandtl number, Pr that is extended to cover the range from 0.01 to 100.

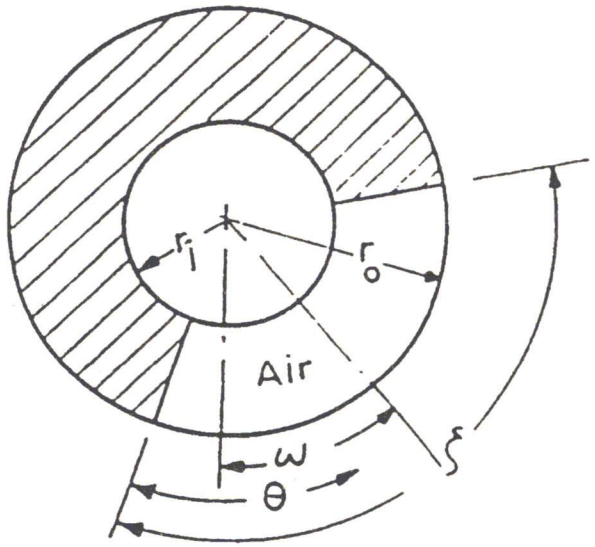

Figure 1. Schematic diagram for the annular segment

Governing Equations

For the problem of two concentric horizontal cylinders, the flow is laminar for $Ra_{di} < 10^8$ [14]. Since the range of Ra in this study will be in this limit, the laminar flow regime will be assumed in the present analysis.

In the present analysis, it is assumed that the flow is steady two dimensional, Newtonian, and has variable fluid properties. It is assumed further that viscous dissipation is negligible, no internal heat generation, and the air in the gap between the two considered isothermal cylindrical arcs as a perfect gas. The Boussinesq approximation is investigated in the results too for sake of comparison.

The governing equations in cylindrical coordinates system are given as follows:

1- *Continuity Equation:*

$$\frac{1}{r}\frac{\partial}{\partial r}(r\,\rho\,v_r)+\frac{1}{r}\frac{\partial}{\partial\theta}(\rho\,v_\theta)=0 \tag{1}$$

2- *Momentum Equations:*

v_r Equation:

$$\frac{1}{r}\frac{\partial}{\partial r}[r(\rho v_r v_r)]+\frac{1}{r}\frac{\partial}{\partial\theta}[(\rho v_r v_\theta)]=\frac{1}{r}\frac{\partial}{\partial r}\left[\left(r\mu\frac{\partial v_r}{\partial r}\right)\right]+$$
$$\frac{1}{r}\frac{\partial}{\partial\theta}\left[\left(\mu\frac{1}{r}\frac{\partial v_r}{\partial\theta}\right)\right]+\left[-\frac{\partial p}{\partial r}+F_r+\frac{\rho v_\theta^2}{r}-\frac{2\mu}{r^2}\frac{\partial v_\theta}{\partial\theta}-\frac{\mu v_r}{r^2}\right] \tag{2}$$

v_θ Equation:

$$\frac{1}{r}\frac{\partial}{\partial r}[r(\rho v_r v_\theta)]+\frac{1}{r}\frac{\partial}{\partial\theta}[(\rho v_\theta v_\theta)]=\frac{1}{r}\frac{\partial}{\partial r}\left[\left(r\mu\frac{\partial v_\theta}{\partial r}\right)\right]+$$
$$\frac{1}{r}\frac{\partial}{\partial\theta}\left[\left(\mu\frac{1}{r}\frac{\partial v_\theta}{\partial\theta}\right)\right]+\left[-\frac{1}{r}\frac{\partial p}{\partial\theta}+F_\theta-\frac{\rho v_r v_\theta}{r}+\frac{2\mu}{r^2}\frac{\partial v_r}{\partial\theta}-\frac{\mu v_\theta}{r^2}\right] \tag{3}$$

3- Energy Equation

$$\frac{1}{r}\frac{\partial}{\partial r}[r(\rho v_r T)]+\frac{1}{r}\frac{\partial}{\partial\theta}[(\rho v_\theta T)]=\frac{1}{r}\frac{\partial}{\partial r}\left[\left(r\rho\alpha\frac{\partial T}{\partial r}\right)\right]+$$
$$\frac{1}{r}\frac{\partial}{\partial\theta}\left[\rho\alpha\frac{1}{r}\frac{\partial T}{\partial\theta}\right] \tag{4}$$

The body forces can be given as follows:

$$F_r=-\rho\,g\sin\psi \qquad F_\theta=-\rho\,g\cos\psi$$

where Ψ, the angle measured from a horizontal plane, is defined as:

$$\psi=\omega-\frac{\pi}{2}-\frac{\zeta}{2}+\theta \tag{5}$$

To write the above equations in dimensionless form, we used the following scales:
d_i^*, α_o / d_i^*, $\rho_o\,\alpha_o^2 / d_i^{*2}$, and $T_h - T_c$ respectively for the length, velocity, pressure and temperature. where:

$$d_i^* = d_i / Ra_{d_i}^{\frac{1}{3}}$$

Before solving the system of equations (1-4) it is convenient to express the governing equations in terms of the general transport equation given in dimensionless form as:

$$\frac{1}{R}\frac{\partial}{\partial R}\left[R\left(\frac{\rho}{\rho_o}V_R\varphi\right)\right]+\frac{1}{R}\frac{\partial}{\partial\theta}\left[\left(\frac{\rho}{\rho_o}V_\theta\varphi\right)\right]=\frac{1}{R}\frac{\partial}{\partial R}\left[\left(R\Gamma_\varphi\frac{\partial\varphi}{\partial R}\right)\right]+\frac{1}{R}\frac{\partial}{\partial\theta}\left[\left(\Gamma_\varphi\frac{1}{R}\frac{\partial\varphi}{\partial\theta}\right)\right]+S_\varphi \quad (6)$$

where S_φ is the linearized source term of the transported variable φ given as:

$$S_\varphi = S_c + S_v \cdot \varphi \quad (7)$$

The corresponding diffusion coefficients and source terms of the governing equations are listed in Table (1).

Table 1. Dimensionless Diffusion Coefficients and Source Terms for the Governing Equations (6).

φ	Γ_φ	S_c	S_v
1	0.0	0.0	0.0
V_R	$Pr\ \frac{\mu}{\mu_o}$	$\left[-\frac{\partial P}{\partial R}-\frac{\rho}{\rho_o}\frac{Pr}{\xi}\sin\psi+\frac{\rho}{\rho_o}\frac{V_\theta^2}{R}-2\frac{\mu}{\mu_o}\frac{Pr}{R^2}\frac{\partial V_\theta}{\partial\theta}\right]$	$-\frac{\mu}{\mu_o}\frac{Pr}{R^2}$
V_θ	$Pr\ \frac{\mu}{\mu_o}$	$\left[-\frac{1}{R}\frac{\partial P}{\partial\theta}-\frac{\rho}{\rho_o}\frac{Pr}{\xi}\cos\psi+2\frac{\mu}{\mu_o}\frac{Pr}{R^2}\frac{\partial V_R}{\partial\theta}\right]$	$-\frac{\rho}{\rho_o}\frac{V_R}{R}-\frac{\mu}{\mu_o}\frac{Pr}{R^2}$
ϑ	$\frac{\alpha}{\alpha_o}\frac{\rho}{\rho_o}$	0.0	0.0

Boundary Conditions

For an annular segment with isothermal inner and outer cylindrical arcs and perfectly insulated sides, the boundary conditions, governing the velocity and temperature variations inside the gap, are prescribed as:

$$V_\theta = V_R = 0,\ \vartheta = 1 \quad \text{at } R = R_i \quad (8)$$

$$V_\theta = V_R = \vartheta = 0 \quad \text{at } R = R_o \quad (9)$$

$$\frac{1}{R}\frac{\partial\vartheta}{\partial\theta} = V_R = V_\theta = 0 \quad \text{at } \theta = 0 \quad (10)$$

$$\frac{1}{R}\frac{\partial\vartheta}{\partial\theta} = V_R = V_\theta = 0 \quad \text{at } \theta = \zeta \quad (11)$$

The average value of Nusselt number $\overline{Nu_{d_i}}$ calculated at the hot surface may take the following form:

$$\overline{Nu_{d_i}} = \frac{\bar{h}d_i}{k} = \frac{Ra_{d_i}^{\frac{1}{3}}}{\zeta}\sum_{\text{hot surface}}\frac{-\partial\vartheta}{\partial R}\cdot\Delta\theta \quad (12)$$

A modified Nusselt number is defined as

$$\overline{Nu^*_{d_i}} = \overline{Nu_{d_i}} \cdot \frac{k}{k_o} = \frac{\bar{h} d_i}{k_o} \qquad (13)$$

3. *Method of solution*

The above equations represent a system of simultaneous nonlinear equations which can not be solved analytically. So, the numerical methods remain the only possible way one could take. The computer program used to solve the above equations is based on the solution of the continuity, momentum, and energy equations with variable fluid properties. The partial differential equations were transformed to finite difference equations by using a central-differencing scheme, except for the convection term which was discretized by using a power-law scheme described in Patankar [24]. For the variable property computations, each property value was updated at each grid point for each iteration. For the constant property computations and for calculating the heat transferred, each property should be evaluated at the cold temperature T_c . The well known SIMPLE algorithm was the scheme used to solve the complete system of equations. For more details of this scheme, see [25].

Grid Design

One of the most important parameters for getting an accurate solution for problems involving convection in enclosures is the grid design and its distribution within the domain of solution. Also the total number of grid points is another factor one must consider when designing any grid system. Based on the two concentric cylinders problem, it was found that a 50 x 40 (r x θ) grid is suitable for getting an accurate solution with a reasonable CPU time as illustrated in Table 2 . The grid distribution was established using a regular-to-irregular grid transformer.

Table 2. Effect of grid density on solution accuracy for $Ra_{d_i} = 5.12 \times 10^5$ & γ=3.5 (Case of Two Concentric Cylinders).

$\theta \times R$	$\overline{Nu_{d_i}}$
30 x 40	9.71
40 x 50	9.72
50 x 60	9.723

Before proceeding with the solution of the problem under investigation, the code was tested for the conduction solution of the problem and the result was found exactly the same as that of the closed form solution $\overline{Nu_{d_i}} = 2 / \ln \gamma$.

4. VALIDATION OF THE BOUSSINESQ APPROXIMATION

Figures (2) show plots of the modified average Nusselt number $\overline{Nu_{d_i}^*}$ calculated at the hot cylinder for ζ = 180°, γ= 2, $10^3 \le Ra_{d_i} \le 10^6$, Pr= 0.71, ω = 0° and 90° for different values of ξ namely 0.2, 0.5, and 1.0, compared to that based on the Boussinesq approximation. For the constant property assumption, the reference temperature used was the outer cylinder temperature T_c, and in order to make a real simulation of the case under investigation, the outer cylinder temperature T_c was taken as 350 K.

The modified Nusselt number is based on a thermal conductivity k_o (at T_o) instead of k(at T_h); this gives an equivalent value of the heat transfer coefficient for all cases (i.e. Boussinesq and other ξ ratios) as the thermal conductivity will be the same in all cases. It is clearly shown that for the conduction regime i.e Ra < 10^4, as ξ increases the heat transfer rate also increases. This is a direct result of the increase of the thermal conductivity without any viscosity effect. By increasing the value

of Ra_{d_i} the flow changes towards the convective regime and as a result the viscosity effect begins to appear and balance the increase of thermal conductivity effect.

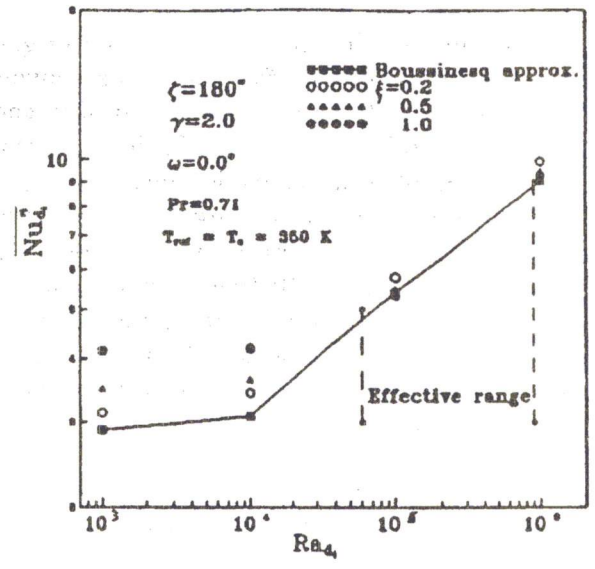

(a)

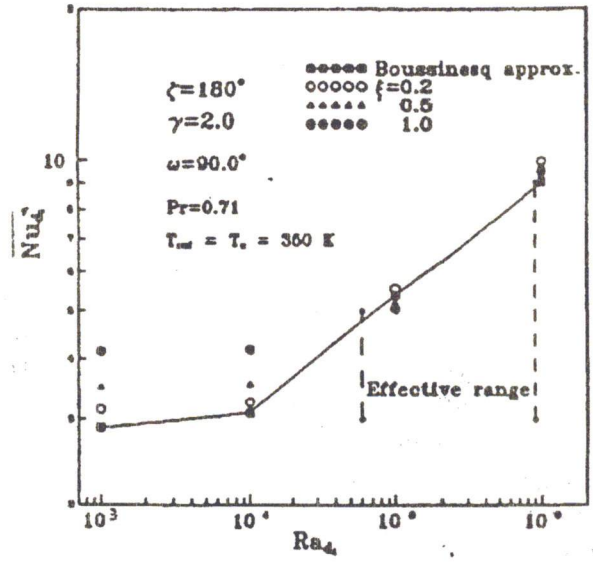

(b)

Figure 2. Heat transfer results with variable properties.

One can easily show that for $5\times10^4 \le Ra_{d_i} \le 10^6$ there is only a slight difference (about 3 %) between the heat rates based on the Boussinesq approximation and the variable properties case. For our problem the increase in Ra_{d_i} is mainly due to the increase of ΔT. As ΔT increases ξ also increases and vice versa. This means that the Boussinesq approximation gives heat transfer rates very close to that of the variable properties case and the error in worst conditions does not exceed 5 %.

Finally we must indicate that the variable properties case takes approximately double the CPU time as that of the Boussinesq approximation, and because of the large number of runs required in the present study, it is reasonable to use the Boussinesq assumption instead of using the variable properties cases.

5. RESULTS AND DISCUSSIONS

Before discussing the heat transfer rates in terms of Nusselt number, it is desirable to examine the energy transfer process in the annular segment and the effect of rotation on this process. Figure (3) represents isotherms (right) and stream lines (left) for the case study data as shown in the figure. Figure (3-a) represents the case of ω =90° and shows streamlines and isotherms very similar to those of two concentric cylinders. For this value of Rayleigh number, the boundary layer is well defined along the inner cylinder and the flow consists of one convective cell filling the entire domain of the gap. The fluid immediately adjacent to the warm inner cylinder rises due to buoyant force with a corresponding increase in the boundary layer thickness. At the top of the inner cylinder, the thermal boundary layer turns around it and also the flow separates forming a thermal plume. The hot up-flowing fluid impinges on the cold outer cylinder surface at the top and is cooled. The fluid descends along the outer cylinder toward the bottom of the annular segment. As the fluid approaches the bottom, it encounters an adverse pressure gradient which forces it to separate away from the outer cylinder and move to the bottom of the inner cylinder. As a result of impinging the hot cylinder, the local heat transfer rate near this region is

expected to be high. This can clearly be observed in Figure (3-a) from the dense isotherms near the top of the outer cylinder and the bottom of the inner cylinder.

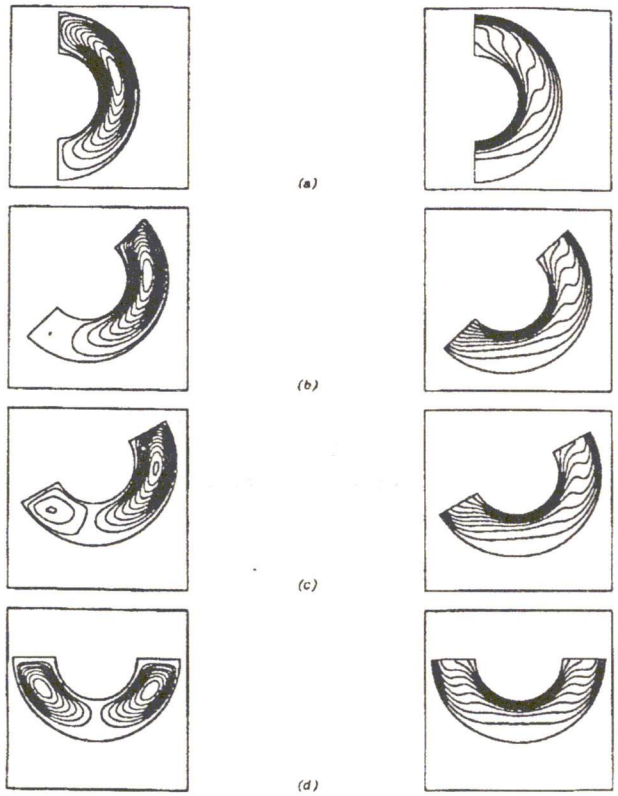

Figure 3. Stream lines and isothermal contours for $Ra_{d_i}=10^5$, $\gamma=2$, (a) $\omega = 90°$, (b) $\omega=45°$, (c) $\omega = 30°$ and (d) $\omega =0°$.

By rotating the annular segment in the clock wise direction, the convective cell advances towards the vertical-like part of the annular segment forming a stagnant dead zone in the bottom left corner of the segment as shown in Figure (3-b). This situation also shows the beginning of formation of another cell. The isotherms at the bottom of the inner cylinder are dense and a high local Nusselt number is also expected there. Rotating the segment more and more the second cell starts to appear more stronger and the right cell more weaker until finally at $\omega =0°$ the two cells are in full symmetry and fill the entire domain.

Figure (4) shows the effect of rotation angle on the average Nusselt number for different radii ratios. As the annular segment rotates, it is clearly shown that the Nusselt number decreases until it reaches a minimum value and then increases again. As the radii ratio γ increases, the value of $\overline{Nu_{d_i}}$ at $\omega = 0°$ decreases while the image is reversed at $\omega = 90°$. The magnitude and location of the minimum $\overline{N\ u_{d_i}}$ change with the angle of rotation. The maximum deviation of the minimum value of $\overline{N\ u_{d_i}}$ from that for the horizontal position ($\omega = 0°$) was for $\gamma =2$. At this value of radii ratio, Nusselt number reaches its minimum value at an angle ω of about 45° . As γ increases the corresponding minimum value of $\overline{N\ u_{d_i}}$ decreases and shifts towards the horizontal position ($\omega= 0$).

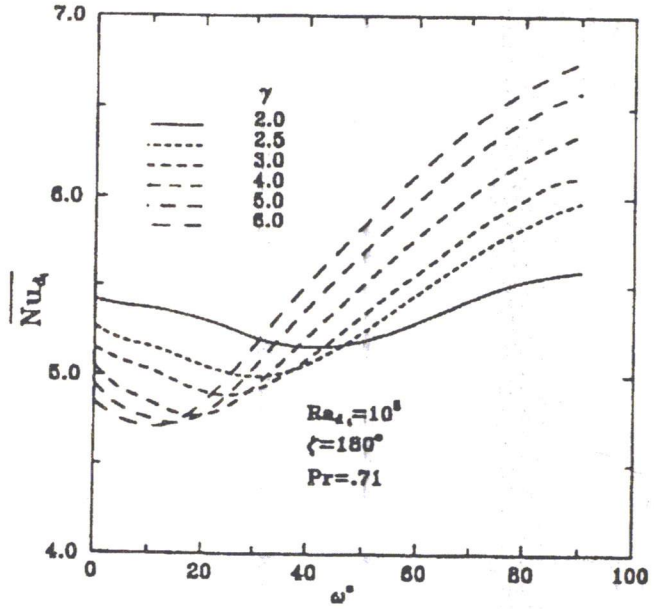

Figure 4. Nusselt number versus rotation angle for different Radii ratios.

Figure (5) shows the influence of the Rayleigh number Ra_{d_i} on Nusselt number $\overline{N\ u_{d_i}}$ for radii ratio $\gamma= 3$ and different rotation angles ω. At $Ra_{d_i} = 10^4$ there is no significant influence of rotation on $\overline{N\ u_{d_i}}$. This is due to the fact that the situation is still very close to the conduction regime. However as Ra_{d_i} increases $\overline{N\ u_{d_i}}$ also increases, and the rotation effect

takes place. The minimum Nusselt number trend begins to appear and its position is almost the same for all Rayleigh numbers. Finally at any value of ω, Nusselt number will be less than that of the two concentric cylinders given in reference [14]. For example at $Ra_{d_i} = 10^5$, $\gamma = 3.0$ and Pr = .71 Hessami et al [14] found $\overline{N u_{d_i}} = 6.26$. As expected the difference between the two cases will be minimum at $\omega = 90^\circ$.

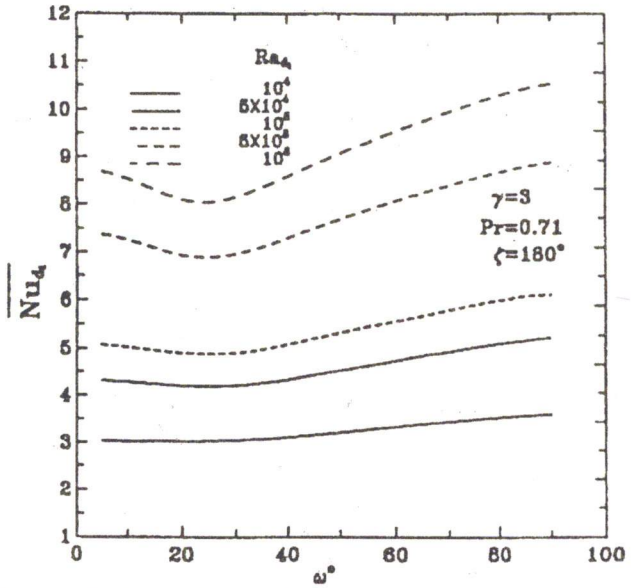

Figure 5. Nusselt number versus rotation angle for different Rayleigh numbers.

Figure (6) represents the effect of changing the annular segment angle ζ on the average Nusselt number for different radii ratios at Ra = 10^5 and $\omega = 0^\circ$. It is shown that by decreasing the segment angle ζ, the average Nusselt number also decreases. As γ increases the difference in average Nusselt number for different values of ζ becomes more clear. The plot for $\zeta = 90^\circ$ is similar to that based on the conduction problem (Nu = 2 / ln γ) giving an indication that the conduction mode is dominating the heat transfer process in the gap. That is, as the thickness of the air gap increases, the thermal resistance, inversely proportional to the heat conductance, increases too. On the other hand, for $\zeta = 240^\circ$ or 300°, the flow is changed to the convection regime. For the convection regime, $\overline{N u_{d_i}}$ is increased with the increase of γ in contrary to the conduction regime.

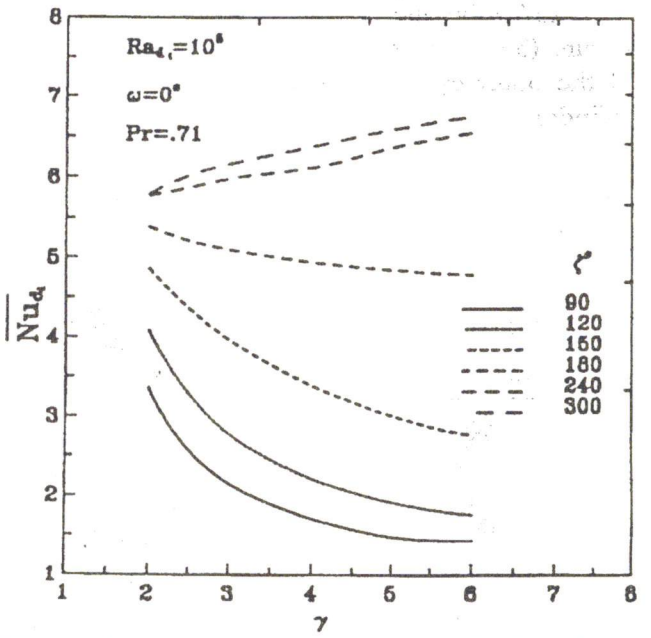

Figure 6. Nusselt number versus Radii ratio for different segment angles.

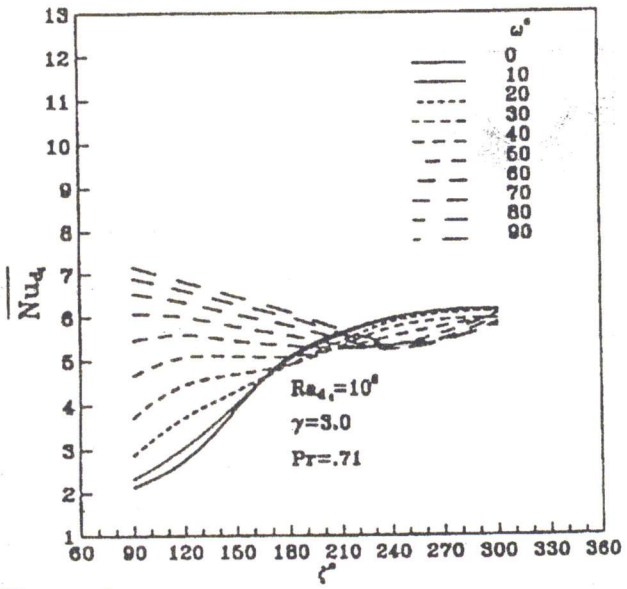

Figure 7. Nusselt number versus segment angle for different Rotation angles.

Figure (7) shows the influence of rotation angle on the average Nusselt number for different segment angles for Ra = 10^5, Pr = 0.71, and $\gamma = 3$. It is shown that as the sector angle increases, the average Nusselt number also increases. This trend remains valid till $\omega = 40^\circ$ after which the image is reversed.

However at $\omega = 90°$ the influence of ζ on $\overline{Nu_{d_i}}$ is opposite to that at $\omega = 0°$.

Finally, Figure (8) represents the influence of Prandtl number on the average Nusselt number for $Ra = 10^5$, $\omega = 90°$ and $\gamma = 3$. For low Pr, (0.01<Pr<1.0), the average Nusselt number increases with a decreasing rate with the increase in Pr. While for high Pr, (Pr>1.0), no significant effect of Pr on Nusselt was observed

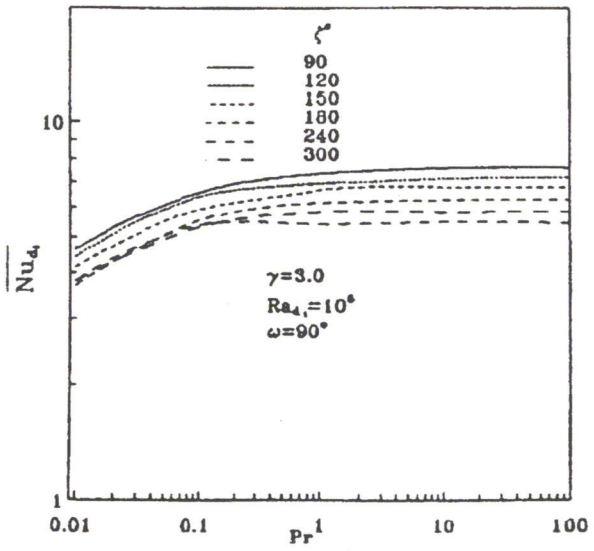

Figure 8. Effect of Prandtl number on Nusselt number for different segment angles.

6. CORRELATIONS

Due to the large amount of runs required to cover all the ranges of variables and the sophisticated trend of each variable on the average Nusselt number, it is very difficult to include all variables in one correlation. We will correlate the average Nusselt number as a function of γ, Ra_{d_i}, and Pr in the form:

$$\overline{Nu_{d_i}} = C_1 Ra_{d_i}^{C_2} \gamma^{C_3} \left(\frac{Pr}{Pr + C_4} \right)^{C_5} \qquad (15)$$

where all the coefficients C_i, i = 1 to 5 will vary for different values of ζ and ω. Table (3) gives the different values of the coefficients as well as the percentage of the mean deviation (MD) in cases where the number of data points was sufficient enough to give a correlation with reasonable accuracy.

The correlations are valid for $10^4 \le Ra_{d_i} \le 10^6 E$, $2 \le \gamma \le 6$ and $.01 \le Pr \le 100$

Acknowledgements

This work was financially supported by the Academy of Scientific Research and Technology, Egypt under project titled " Utilization of Solar Energy in the temperature range 100- 400 °C "

Nomenclatures

d	diameter
d_i^*	modified diameter, $d_i / Ra_{di}^{1/3}$
g	gravitational acceleration
h	coefficient of heat transfer
k	thermal conductivity
Nu	Nusselt number
P	pressure
Pr	Prandtl number
R	dimensionless radius, r/d_i^*
Ra_{di}	Rayleigh number based on inner diameter
Ra	Rayleigh number based on gap width
r	radius
S	source term
T	temperature
V	dimensionless velocity, $V d_i^* / \alpha_o$
v	velocity

Greek

α	thermal diffusivity
β	coefficient of thermal expansion
Γ	diffusion coefficient
γ	radii ratio
ζ	sector angle
μ	dynamic viscosity
ν	kinematic viscosity
φ	transported quantity
ψ	angle defined in Equation (5)
ξ	dimensionless temperature ratio, $(T_h - T_c)/T_c$
ρ	density
ω	rotation angle
ϑ	dimensionless temperature, $(T - T_c) / (T_h - T_c)$

Table 3. Constants for Equation (15).

ω^o	ζ^o	C_1	C_2	C_3	C_4	C_5	M D %
0.0	90	2.878	.05768	-.800	0	0	3.95
0.0	120	1.935	.11623	-0.854	0	0	0.9
0.0	150	.865	.18771	-.5768	0	0	0.5
0.0	180	.3711	.23527	-.0786	0	0	0.64
0.0	240	.31309	.24243	.14571	0	0	0.125
0.0	300	.31694	.2435	.15185	0	0	0.8
15	180	.45634	.21872	- .1110	0	0	0.31
30	180	.43827	.21112	.0046	0	0	0.2
45	180	.35933	.22398	.0957	0	0	0.27
60	180	.33859	.23091	.13277	0	0	0.066
75	180	.3387	.23406	.14618	0	0	0.125
90	180	.34087	.23569	.15427	0	0	0.354
90	90	.35767	.25201	.14405	.93516	.068	0.053
90	120	.38866	.23734	.15326	.064	.2331	0.47
90	150	.39538	.23199	.14725	.0866	.2134	0.089
90	180	.35479	.23386	.16455	.11224	.19293	1.637
90	240	.23997	.2606	.068	.043	.231	1.648
90	300	.22713	.22713	.0455	.0518	.24158	0.277

Subscripts

c cold
h hot
i inner
o outer
r, R radial direction
θ angular direction

REFERENCES

[1] T.H. Kuehn and R.J. Goldstein, An experimental and theoretical study of natural convection in the annulus between horizontal concentric cylinders, *J. Fluid Mech.* 74, pp. 695-719, 1976.

[2] B. Farouk and S.I. Güceri, Laminar and turbulent natural convection in the annulus

between horizontal concentric cylinders, *J. Heat Transfer*, 104, pp. 631-636, 1982.

[3] L.S. Yao, Analysis of heat transfer in slightly eccentric annuli, *J. Heat Transfer*, 102, pp. 279-284, 1980.

[4] M. Singh and S.C. Rajvanshi, Heat transfer between eccentric rotating cylinders, *J. Heat Transfer*, 102, pp. 347-350, 1980.

[5] C.H. Cho, K.S. Chang and K. H. Park, Numerical simulation of natural convection in concentric and eccentric horizontal annuli, *J. Heat Transfer*, 104, pp. 624-630, 1982.

[6] J. Prusa and L.S. Yao, Natural convection heat transfer between eccentric horizontal cylinders, *J. Heat Transfer*, 105, pp. 108-116, 1983.

[7] D.N. Mahony, R. Kumar and E. H. Bishop, Numerical invesyigation of variable property effects on laminar natural convection of gases between two horizontal isothermal concentric cylinders, *J. Heat Transfer*, 108, pp. 783-789, 1986.

[8] M.A. Hessami, A. Polard and R.D. Rowe, Numerical calculations of natural convection heat transfer between horizontal concentric isothermal cylinders-effect of variation of fluid properties, *J. Heat Transfer*, 106, pp. 668-671, 1984.

[9] R. Kumar, Study of natural convection in horizontal annuli, Int. *J. Heat Mass Transfer*, 31, pp. 1173-1148, 1988.

[10] S.R.M. Gardiner and R.H. Sabersky, Heat transfer in annular gap, Int. *J. Heat Mass Transfer*, 21, pp. 1459-1466, 1978.

[11] L.S. Yao and F.F. Chen, Effects of Natural convection in the region around a heated horizontal cylinder, *J. Heat Transfer*, 102, pp. 667-672, 1980.

[12] T.H. Kuehn and R.J. Goldstien, A parametric study of Prandtl number and diameter ratio effects on natural convection heat transfer in horizontal cylindrical annuli, *J. Heat Transfer*, 102, pp. 768-770, 1980.

[13] M.C. Charrier-Mojtabi A. Mojtabi and J.P. Caltagirone, Numerical solution of a flow due to natural convection in horizontal cylindrical annuli, *J. Heat Transfer*, 101, pp. 171-173, 1979.

[14] M.A. Hessami, A. Pollared, R.D. Rowe and D.W. Ruth, A study of free convection heat transfer in a horizontal annulus with a large radii ratio, *J. Heat Transfer*, 107, pp. 747-754, 1984.

[15] Y. Rao, Y. Miki, K. Fukuda and Y. Takata, Flow patern of natural convection in horizonyal cylindrical annuli, Int. *J. Heat Mass Transfer*, 28, pp. 705-714, 1985.

[16] R.E. Powe, C.T. Carley and E.H. Bishop, Free convective flow patterns in cylindrical annuli, *J. Heat Transfer*, 91, pp. 310-314, 1969.

[17] Y. Takata, K. Iwashige, K. Fukuda and S. Hasegawa, Three-dimensional natural convection in an inclined cylindrical annulus, Int. *J. Heat Mass Transfer*, 27, pp. 747-754, 1984.

[18] P. Vasseur, L. Robillard and B. Chandra Shekar, Natural convection heat transfer of water within a horizontal cylindrical annulus with density inversion effects, *J. Heat Transfer*, 105, pp. 177-123, 1983.

[19] E. Van De Sande and B. J. G. Hamer, Steady and transient natural convection in enclosures between horizontal circular cylinders (constant heat flux), Int. *J. Heat Mass Transfer*, 22, pp. 361-370, 1979.

[20] Y.T. Sui and B. Tremblay, On transient natural convection heat transfer in the annulus between concentric, horizontal cylinders with isothermal surfaces, *Int. J. Heat Mass Transfer*, 27, pp. 103-111, 1984.

[21] S.S. Kwon, T.H. Kuehn T.S. Lee, Natural convection in the anuulus between horizontal circular cylinders with three axial spacers, *J. Heat Transfer*, 104, pp. 118-124, 1982.

[22] S.S. Kwon and T. H. Kuehn, Conjugate natural convection heat transfer from a horizontal cylinder with a long vertical longitudinal fin, *Num. Heat Transfer*, 6, pp. 85-102, 1983.

[23] H.Q. Yang, K.T. Yang and J.R. Lloyd, Natural convection suppression in horizontal annuli by azimuthal baffles, Int *J. Heat Mass Transfer*, 31, pp. 2123-2135, 1988.

[24] S.V. Patankar, A calculation procedure for two-dimensional elliptic situations, *Num. Heat Transfer*, vol. 2, 1979.

[25] S.V. Patankar, *Numerical heat transfer and fluid flow*, McGraw-Hill

[26] D.A. Anderson, J.C. Tannehill and R.H. Pletcher, *Computational fluid mechanics and heat transfer*. McGraw-Hill.